INSTITUTE FOR FUSION STUDIES

Reynolds Stress of Localized Toroidal Modes

Y.Z. ZHANG
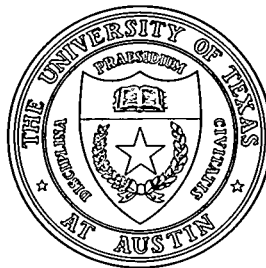International Center for Theoretical Physics
Miramore, Trieste, Italy
and
S.M. MAHAJAN
Institute for Fusion Studies
The University of Texas at Austin
Austin, Texas 78712

THE UNIVERSITY OF TEXAS

AUSTIN

DISCLAIMER

**Portions of this document may be illegible
in electronic image products. Images are
produced from the best available original
document.**

Reynolds Stress of Localized Toroidal Modes

Y.Z. Zhang

International Center for Theoretical Physics, Miramore, Trieste, Italy

and

S.M. Mahajan

Institute for Fusion Studies, The University of Texas at Austin

Austin, Texas 78712

Abstract

An investigation of the 2D toroidal eigenmode problem reveals the possibility of a new consistent 2D structure, the dissipative BM-II mode. In contrast to the conventional ballooning mode, the new mode is poloidally localized at $\pi/2$ (or $-\pi/2$), and possesses significant radial asymmetry. The radial asymmetry, in turn, allows the dissipative BM-II to generate considerably larger Reynolds stress as compared to the standard slab drift type modes. It is also shown that a wide class of localized dissipative toroidal modes are likely to be of the dissipative BM-II nature, suggesting that at the tokamak edge, the fluctuation generated Reynolds stress (a possible source of poloidal flow) can be significant.

I. INTRODUCTION

For a tokamak-like magnetically confined plasma, the macroscopic radial equilibrium is obtained by balancing the radial components of the outward ∇P force with the inward pinching force $\mathbf{J} \times \mathbf{B}$. Because the surface average of the poloidal projection of these two forces is zero, they play no part in the poloidal force-balance. The plasma dynamics in the poloidal direction, therefore, is controlled by the remaining terms, *e.g.*, the inertial (convective), the viscosity, and possibly the dissipative terms in the equation of motion. Since the perpendicular viscosity is rather small for a strongly magnetized plasma, and the surface averaged inertial and gyroviscosity terms are also zero (for the principal perpendicular motion consisting of the $\mathbf{E} \times \mathbf{B}$ drift and the diamagnetic flow), the parallel viscosity survives as the only significant force in the poloidal direction. The dissipative nature of this term would then imply that a steady poloidal flow will not be sustained by a tokamak-like plasma.

This understanding of the poloidal force balance, however, is inconsistent with recent experiments on L-H transitions, where it is seen that large poloidal flows appear along with the onset of the transition.[1] There surely must exist a force which drives and sustains the observed poloidal flows in high confinement plasma configurations. What is it?

Many theories have been devised to answer this important question. Among others, the poloidal torque given by the radial gradients of the Reynolds stress [the inertial term constructed from the *fluctuating* plasma motions (fields)] has been considered as one of the possible forces driving the poloidal flow. While the original physical mechanism related to this issue was investigated by Berk and Molvig,[2] Diamond and Kim[3] were the first to publish an estimate for the magnitude of the poloidal torque resulting from the fluctuating slab-model drift waves. It was also claimed that this estimate was consistent with the DIII-D experiment. Making use of the same slab drift wave model, however, has led us to much

smaller estimates. For comparison, the details of our calculation are presented in Sec. II. It is highly possible that, in their estimate, Diamond and Kim have missed that the overall radial energy flow is vastly lowered by the 'pairing' mechanism — there is a major cancellation because two waves peaking at adjacent rational surfaces contribute oppositely to the radial energy flow in the intervening region.

For the 'pairing' cancellation to be negligible, the mode structure must possess substantial radial asymmetry so that there is a net energy flow in a well defined radial (inward or outward) direction from all the contributing modes. Notice that a simple real displacement of the mode from the rational surface will not lead to such a desired property.

Within the framework of slab model the intrinsic asymmetry can be acquired, if and only if the driving force (or a part of it) is odd on reflection about the rational surface. The basic mode equation, in that case, will have mixed parity because other terms are, generally, even on reflection. Admittedly, there are a few slab modes such as the drift-rippling mode and the parallel flow shear driven mode, satisfying this condition. Recently, Dong et al.[4] calculated the Reynolds stress of the parallel flow shear driven mode. Their manipulation of averaging the Reynolds stress over the 'microscopic scale' turns out to be qualitatively equivalent to realizing the 'pairing' mechanism. The analysis presented in Sec. II of the present paper (not a trivial replica of their calculation) indicates that the Reynolds stress is indeed greatly enhanced by the intrinsic asymmetry due to the odd-parity drive. However, by no means, does it follow, that a significant Reynolds stress in a tokamak can arise only from modes of mixed parity. The modes in a tokamak are intrinsically two dimensional (2D) [throughout this paper we only consider the axisymmetric tori. The toroidal mode number n is thus treated as a good quantum number], and an effective radial asymmetry can be 'created' as a result of this 2D structure.

For the 2D toroidal mode localized at a rational surface, the eigenmode equation is no longer invariant under 'reflection' with respect to the rational surface. To the lowest

3

order, it may still conserve what we term the combined parity (CP) — invariance under a simultaneous 'reflection' and poloidal inversion. If the mode structure has this symmetry, it is straightforward to show that the mode envelope is radially symmetric about the rational surface, and also possesses the up-down symmetry in the poloidal cross section. Therefore, a radial asymmetry for the localized toroidal modes must arise from the CP violation (if any) of mode structure. It will be shown later that the 2D mode structure is not determined by the lowest order equation (known to conserve CP), but by higher order equations which may or may not be invariant under CP. To determine whether these 2D structures will have considerable radial asymmetry (and hence allow a build-up of significant Reynolds stress), we must thoroughly investigate the very nature of the eigenmodes on an axisymmetric torus.

For historical reasons, the theoretical frameworks developed to study the structure of the 2D localized eigenmodes are collectively called the ballooning theory. The ballooning theory is an active area of research, and its plentiful literature is not easily accessible to a normal reader. One of the tasks of this paper is to describe and explain crucial aspects (some recently discovered) of the theory in simple language. Naturally, we will spend more time on those aspects which are of direct relevance to the current effort.

The derivations and details of the theory will be dealt with in the main body of the text (Sec. III). In the introduction, we shall give only qualitative description of the salient features. For most of its history, the ballooning theory concentrated on a particular structure of the 2D localized toroidal eigenmode which is localized at the poloidal angle $\vartheta = 0$ (or $\vartheta = \pi$).[5] For this structure, to be called BM-I [the ballooning mode of the first kind], the CP is conserved making it an unlikely candidate to yield significant Reynolds stress. Therefore, the structure of BM-I will not be discussed to detail in this paper.

A few years ago, a novel structure was discovered in course of the attempts: 1) to derive the continuum damping of toroidal Alfvén eigenmode (TAE),[6-9] and 2) to resolve the difficulties associated with the BM-I structure for the dissipative systems.[10-11] There are

4

three generic features that distinguish the new structure of BM-II [the ballooning mode of the second kind] from the earlier BM-I: (a) For a given toroidal mode number BM-II may occur for any plasma profile and at all radii. This is in contrast to BM-I, whose occurrence is subject to the solvability condition, and may be restricted to very limited radial locations, (b) The 2D eigenvalue is approximately given by the average of the λ-parameterized eigenvalues of the ballooning equation [the lowest order equation in the ballooning theory is called the ballooning equation. In the ballooning equation, the angle like variable λ (ϑ_k according to some authors), which is the Fourier conjugate of the poloidal mode number l [see Eq. (12)], appears only as a parameter. Higher order equations are differential equations in λ.]. This is in contrast to BM-I, for which the 2D eigenvalue is essentially the λ-parameterized eigenvalue of the ballooning equation evaluated at $\lambda = 0$ (or $\lambda = \pi$), save for some very special cases,[10] (c) The poloidal structure of BM-II is not localized at $\vartheta = 0$ (or $\vartheta = \pi$). [It is worth mentioning that the BM-I and the BM-II have also been called by Dewar,[12] the 'trapped mode' and the 'passing mode' respectively]. This last feature (c) of the BM-II structure is not yet fully documented in the literature. If appropriate consistency constraints can be satisfied, the BM-II can take totally distinct forms for the dissipative and the non-dissipative systems. For non-dissipative systems (like the TAE), there is no poloidal localization, *i.e.*, the mode does not balloon at all.[8] For this structure (requires an additional small parameter for consistency), the CP violation is weak, and there is no obvious source for radial asymmetry. Thus, the non-dissipative BM-II is also unlikely to be a source for generating significant Reynolds stress.

The situation can altogether change for the dissipative systems. In Sec. III, it will be shown that for a λ-parameterized eigenvalue expressed by $\Omega_n(\lambda) = \overline{\Omega}_n + \Delta\Omega_n \cos\lambda$ [cf. Eq. (18)], the existence of finite (not too small) dissipation can cause BM-II to localize at $\lambda = \pi/2$ (or $\lambda = -\pi/2$), and that this localization in λ results in the poloidal localization at $\vartheta = -\pi/2$ (or $\vartheta = \pi/2$). Thus the dissipative BM-II (as distinct from the non-dissipative

mode) is a genuine ballooning mode, has no up-down symmetry in the poloidal plane, and is characterized by strong CP-violation. It is also shown in Sec. III that the λ-localization of the dissipative BM-II (equivalent to the radial localization in the framework of the ballooning theory) is necessary for the validity of applying the ballooning approach to a wide class of dissipative systems that do not have an intrinsic small parameter like the inverse aspect ratio for the TAE. *Therefore, for such a wide class of dissipative systems, the radially localized toroidal mode must possess substantial radial asymmetry, which would lead to a significant Reynolds stress.*

The explicit expression for the 2D structure of dissipative BM-II is derived in Sec. III, where we also include a systematic and self-contained exposition of the ballooning theory formalism in terms of the 2D ballooning transform. The derived expression can be readily used for calculating the Reynolds stress when the solution of the ballooning equation at $\lambda = \pm\pi/2$ is obtained. In Sec. IV we adopt a model equation governing toroidal drift waves for illustrating the calculation of Reynolds stress. The result is then compared with the slab drift-wave calculation of Sec. II, indicating a great enhancement of the Reynolds stress owing to the large radial asymmetry of the 2D mode. Section V is devoted to discussion and concluding remarks.

II. THE REYNOLDS STRESS — SLAB MODES

The poloidal torque induced by Reynolds stress is defined by $T_q \equiv \rho \left\langle \mathbf{e}_\vartheta \cdot (\tilde{\mathbf{u}} \cdot \nabla)\tilde{\mathbf{u}} \right\rangle$, where ρ is the mass density, $\tilde{\mathbf{u}}$ is the fluctuating fluid velocity, $\mathbf{e}_\vartheta$ is the unit vector in the poloidal direction, and $\langle \cdots \rangle$ stands for the ensemble average. Throughout this paper the standard quasi-toroidal coordinate system (r, ϑ, ζ) is adopted. As an example, the fluctuating flow $\tilde{\mathbf{u}} = (c/B^2)\mathbf{B} \times \nabla\varphi$ will be restricted to the direction perpendicular to the equilibrium magnetic field $\mathbf{B}$, where φ is the fluctuating electrostatic potential, $B \equiv |\mathbf{B}|$, and c is the speed of light. This representation corresponds to the cold ion limit, when the contribution

6

from the (warm) ion diamagnetic flow is neglected. The surface averaged torque is found to be well approximated by

$$\langle T_q(r)\rangle_\vartheta = -\frac{\rho c^2}{rB^2}\frac{\partial}{\partial r}\left\langle\oint d\vartheta\,\frac{\partial\varphi}{\partial\vartheta}\frac{\partial\varphi}{\partial r}\right\rangle \equiv -\frac{\rho c^2}{B^2}\frac{\partial\mathcal{R}(r)}{\partial r}, \qquad (1)$$

where $\mathcal{R}(r)$ is the Reynolds stress at the radial position r.

A similar expression also applies to the 'magnetic Reynolds stress' ($\mathcal{R}^{(m)}$), which is associated with the torque induced by the fluctuating magnetic fields, $T_q^{(m)} \equiv -\left\langle e_\vartheta\cdot(\tilde{\mathbf{B}}\cdot\nabla)\tilde{\mathbf{B}}\right\rangle/4\pi$. For $\tilde{\mathbf{B}} = \mathbf{B}\times\nabla\psi/B$, where ψ is the fluctuating magnetic flux,

$$\langle T_q(r)\rangle_\vartheta = -\frac{1}{4\pi r}\frac{\partial}{\partial r}\left\langle\oint d\vartheta\,\frac{\partial\psi}{\partial\vartheta}\frac{\partial\psi}{\partial r}\right\rangle \equiv -\frac{1}{4\pi}\frac{\partial\mathcal{R}^{(m)}(r)}{\partial r}, \qquad (2)$$

In this section the Reynolds stress, due to only the electrostatic slab drift waves, is discussed.

Introducing the relative coordinate to the jth rational surface by $x_j \equiv r - r_j$, and the y coordinate by $dy = rd\vartheta$, one can readily write the amplitude of the slab drift wave peaking at the jth rational surface as

$$\varphi_j(x_j, y, t) = \varphi(r_j)\left\{\exp\left[-i\alpha x_j^2/2\rho_s^2 + ik_y y - i\omega_{k_y}t + i\delta(r_j)\right] + \text{c.c.}\right\}, \qquad (3)$$

where $\omega_{k_y} \equiv (\omega_e^* - i\omega_s)/(1 + k_y^2\rho_s^2 - i\delta_e)$, $\alpha \equiv \omega_s/\omega_{k_y} \approx (\omega_s/\omega_e^*)[1 - i(\delta_e - \omega_s/\omega_e^*)]$, for $k_y\rho_s < 1$ and $\omega_s/\omega_e^* < \delta_e < 1$, $\omega_s \equiv \rho_s c_s k_y/L_s$, L_s is the shear length, ρ_s is the ion Larmor radius at the electron temperature, c_s is the ion sound speed, ω_e^* is the electron diamagnetic frequency, $\delta(r_j)$ is the random phase associated with the wave peaking at the jth rational surface, $\varphi(r_j)$ is the mode (real) amplitude at r_j, and all parameters such as ω_e^*, ρ_s, are associated with the radial position r_j. It is then straightforward to obtain the contribution from the jth rational surface to $\mathcal{R}$,

$$\mathcal{R}_j(r) = \frac{k_y}{2}\left(\frac{d\delta_p}{dr}\right)\varphi^2(r_j)\exp(\text{Im}\,\alpha x_j^2/\rho_s^2), \qquad (4)$$

7

where $\delta_p \equiv - \operatorname{Re} \alpha x_j^2/2\rho_s^2 = -(\omega_s/2\omega_e^* \rho_s^2)x_j^2$.

A few remarks on Eq. (4) are in order. First, the factor $d\delta_p/dr$ represents the phase shift of $\partial\varphi/\partial r$ with respect to φ. If $\partial\varphi/\partial r$ were in phase with φ, while $\partial\varphi/\partial\vartheta$ is 90° phase shifted with respect to φ, the ensemble average of the product $(\partial\varphi/\partial r)(\partial\varphi/\partial\vartheta)$ would be zero. It indicates that not only a zero δ_p, but also a constant δ_p would result in zero Reynolds stress. Second, the phase shift $d\delta_p/dr(\approx x_j)$ has odd parity about the rational surface. Physically, the drift wave energy is generated at the rational surface, and propagates away on both sides (outgoing boundary conditions). If the energy flow is positive on the right side, it is negative on the left side. Thus, on the right side of the jth rational surface the energy flow from the mode peaking at the jth surface will be cancelled by that coming from the mode peaking at the $(j + 1)$th rational surface, if $\mathcal{R}_j$ is antisymmetric with respect to x_j. This is indeed the case for the slab drift waves. However, this cancellation is not complete, because the wave amplitude and the equilibria vary from one to the other rational surface. This cancellation is named as 'pairing' by Berk.[13]

The effect from 'pairing' can be calculated by summing up the contribution from all rational surfaces. Under the approximation

$$\sum_j \mathcal{R}_j \approx \int dr_j(nq\widehat{s}/r_j)\mathcal{R}_j = \int dr_j k_y \widehat{s}\mathcal{R}_j, \tag{5}$$

where $\widehat{s}$ is the magnetic shear at r_j, it yields

$$\mathcal{R}(r) = \sum_j \mathcal{R}_j(r) = -\tfrac{1}{2}\int_{-\infty}^{+\infty} dr_j \left(\frac{\omega_s k_y^2 \widehat{s}}{\omega_e^* \rho_s^2}\right) \varphi^2(r_j)(r - r_j)\exp\left[\operatorname{Im}\alpha(r - r_j)^2/\rho_s^2\right]$$

$$= -\frac{\sqrt{\pi}}{4}\frac{\partial}{\partial r}\left(\frac{\rho_s^2}{\operatorname{Im}\alpha}\sqrt{\frac{\rho_s^2}{|\operatorname{Im}\alpha|}}\frac{\omega_s k_y^2 \widehat{s}}{\omega_e^* \rho_s^2}\varphi^2(r)\right), \tag{6}$$

where use is made of the assumption that the mode width $\Delta_r \equiv \rho_s/\sqrt{|\operatorname{Im}\alpha|/2}$ is much smaller than the equilibrium scale lengths.

The poloidal torque corresponding to Eq. (6) is

$$T_{q[s]}(r) = -\frac{\rho c^2}{B^2}\frac{\partial \mathcal{R}}{\partial r} \approx \sqrt{\frac{\pi}{2}}\frac{\rho c^2}{8B^2}\left(\frac{\Delta_r}{L_f}\right)^2 (\Delta_r k_y \hat{s})\frac{L_n k_y}{L_s \rho_s^2}\varphi^2, \qquad (7)$$

where L_n is the density gradient length, and L_f is the scale length measuring the fastest variation among the equilibrium and the amplitude of the mode envelope.

We can now compare our results with those of Diamond and Kim in Ref. [3]. Making use of their estimates for $\hat{\varphi} \equiv e\varphi/T_e \approx \sqrt{L_s/L_n}\,\rho_s/L_n$, and for the radial current $J_r = nec_s(\rho_s^2/L_n^2)k_y\rho_s$ coupled with the relation $J_r \to cT_q/B$, one can infer that $T_{q[DK]} = (c/B)^2\rho k_y(L_n/L_s)\varphi^2/\rho_s^2$. It is readily seen that the torque given by Eq. (7) is about $(\Delta_r/L_f)^2$ times smaller than $T_{q[DK]}$ in magnitude. Because Δ_r/L_f is much smaller than unity, the poloidal torque derived from a consistent treatment of the slab drift waves is too small to be comparable with the DIII-D experiments.

Recently, Dong et al.[4] studied the Reynolds stress of the mode driven by parallel flow shear. It is interesting to note that this mode has intrinsic asymmetry for the warm ion scenario. In the cold ion limit, however, the mode structure reduces to a real displacement from the rational surface, and energy flow to the right and to the left become almost the same in magnitude. In order to illustrate the effect of the asymmetry, let us consider the following form

$$\varphi_j(x_j, y, t) = \overline{\varphi}(r_j)\left\{\exp\left[-i\alpha(x_j + \Delta_j)^2/2\rho_s^2 + ik_y y - i\omega_{k_y}t + i\delta(r_j)\right] + \text{c.c.}\right\}, \qquad (8)$$

where $\Delta_j \equiv -\rho_s\hat{V}_\parallel'\hat{\omega}/2s(\hat{\omega}+K)$, $\hat{V}_\parallel' \equiv (L_n/c_s)dV_\parallel/dr)$, $s \equiv (L_n/L_s)$, $K \equiv (1+\eta_i)/\tau$, τ is the ratio of the electron to the ion temperature, η_i is the ratio of the ion temperature gradient to the ion density gradient, and $\alpha \equiv \omega_s/\omega_{k_y} = (\omega_s/\omega_e^*)/\hat{\omega}$. The Reynolds stress from the jth rational surface is given by

$$\mathcal{R}_j(r) = \frac{k_y}{2}\left(\frac{d\delta_p}{dr}\right)\varphi^2(r_j)\exp(\text{Im}\,\alpha z_j^2/\rho_s^2), \qquad (9)$$

where $\delta_p \equiv -\operatorname{Re}\alpha(x_j + \operatorname{Re}\Delta_j)^2/2\rho_s^2 + \operatorname{Im}\alpha\operatorname{Im}\Delta_j(x_j + \operatorname{Re}\Delta_j)/\rho_s^2$, and $z_j \equiv x_j + \operatorname{Re}\Delta_j + \operatorname{Re}\alpha\operatorname{Im}\Delta_j/\operatorname{Im}\alpha$, and $\varphi(r_j)$ is the maximum value of the mode peaking at the jth rational surface. The asymmetry of energy flow is obvious from Eq. (9). The leading asymmetry arises from the factor $\operatorname{Re}\alpha\operatorname{Im}\Delta_j/\operatorname{Im}\alpha$, because the contribution from $\operatorname{Im}\alpha\operatorname{Im}\Delta_j$ is small. The total stress is obtained by summing over all the rational surfaces

$$\mathcal{R}(r) = \sum_j \mathcal{R}_j(r) = \frac{1}{2}\sqrt{\frac{\pi\rho_s^2}{|\operatorname{Im}\alpha|}}\frac{\operatorname{Im}\Delta_j[\operatorname{Re}\alpha]^2 k_y^2 \hat{s}}{\operatorname{Im}\alpha\rho_s^2}\varphi^2(r). \tag{10}$$

Compared to Eq. (6), it is greater by the factor ($\hat{\gamma}$ is the growth rate normalized to ω_e^*).

$$(\operatorname{Im}\Delta_j L_f/\rho_s^2)\operatorname{Re}\alpha \approx \frac{\hat{V}_\parallel' K\hat{\gamma}L_f}{2(1+K)^2\rho_s}, \tag{11}$$

which could be much greater than unity for warm ions ($K \approx \mathcal{O}(1)$), implying that the intrinsic radial asymmetry due to odd-parity driving results in great enhancement of the generated Reynolds stress. In the cold ion limit, however, $K = 0$, and $\operatorname{Im}\Delta_j = 0$, so that the intrinsic asymmetry vanishes, and the poloidal torque reduces to the value given by Eq. (7).

From the preceding analysis, we must not conclude that a significant poloidal torque, if there is any in tokamaks, necessarily owes its origin to modes of this or similar description (like the drift-rippling mode with its slab mode structure skewed around the rational surface). This conclusion, as we shall demonstrate in the following sections, is not necessarily true.

III. TOROIDAL MODE STRUCTURE — BALLOONING THEORY

The ballooning theory, in a general sense, is an asymptotic theory for high toroidal mode number (n) fluctuations in an axisymmetric torus. A proper understanding of the mode structure necessitates going beyond the lowest order theory contained in the well-known ballooning equation. (It is again for historic reasons that the lowest order equation of the formulation is called the ballooning equation). We adopt here the rigorous and self-contained

10

formalism based on the so-called 2D ballooning transform.[8−11] This choice is dictated not only by the abstract virtues of brevity and clarity, but also by its demonstrated success in calculating quite sophisticated higher order effects such as the continuum damping of TAE.[9]

In the quasi-toroidal coordinates (r, ϑ, ζ), the toroidal mode (with mode number n) associated with the rational surface r_0 is represented by

$$\varphi_n(r, \vartheta, \zeta) = \exp(in\zeta - im\vartheta) \sum_l \phi_{n,l}(r) \exp(-il\vartheta), \tag{12}$$

where $m \equiv nq(r_0)$, and the integer l labels the sidebands coupled to the central Fourier mode m. The 2D ballooning transform $x \equiv n[q(r) - q(r_0)]$,

$$\phi_{n,l}(r) \equiv \oint d\lambda dk \exp[ik(x - l) - il\lambda]\widehat{\varphi}_n(k, \lambda), \tag{13}$$

represents the 2D wave function $\phi_{n,l}(r)$ (with a continuous variable r and a discrete variable l) in terms of the new 2D wave functions $\widehat{\varphi}_n(k, \lambda)$ labelled by the continuous variables $k(-\infty, +\infty)$, and $\lambda(0, 2\pi)$. This transformation, Eq. (13), is mathematically sound and invertible. In particular, the discrete variable l has been conveniently represented by a continuous, but periodic, variable λ defined on a finite interval $0 - 2\pi$. Because Eq. (13) is a well-defined transformation, the original 2D equation for $\phi_{n,l}(r)$ can be unambiguously transformed to a 2D equation determining $\widehat{\varphi}_n(k, \lambda)$, and vice-versa. In the large n limit, the equation obeyed by $\widehat{\varphi}_n(k, \lambda)$ allows a *formal* asymptotic expansion of the form[10]

$$\left[L_0 + i\frac{L_1}{n}\frac{\partial}{\partial \lambda} + \frac{L_2}{n^2}\frac{\partial^2}{\partial \lambda^2} + \cdots - \Omega \right] \widehat{\varphi}_n(k, \lambda) = 0, \tag{14}$$

where L_0 is the 'ballooning operator', *i.e.*,

$$[L_0 - \Omega_n(\lambda)]\mathcal{X}_n(k, \lambda) = 0 \tag{15}$$

is the ballooning equation, $\Omega_n(\lambda)$ is the λ-parameterized eigenvalue, the operators $L_0, L_1, L_2 \ldots$ usually contain $\partial/\partial k$, but not $\partial/\partial \lambda$, and Ω is the eigenvalue of the 2D system. Generally,

11

tedious but straightforward algebraic manipulations are needed to derive Eq. (14) from the full 2D original equation [the radial variable r is first transformed to x, which is then rewritten as $x = (x \neg l) + l$, whereupon $(x - l)$ is transformed to $i\partial/\partial k$ and l transformed to $-i\partial/\partial\lambda$]. However, for most model equations that have been used for the study of higher order ballooning theory, the derivation of Eq. (14) is quite trivial. In all these examples, the putative operators $L_1, L_2 \dots$ are approximated by $c - numbers$ [for example, see the derivation of Eq. (33) from Eq. (32) in Sec. IV].

The ballooning equation embodies two leading order basic symmetries of the original 2D eigenmode equation. The ballooning operator L_0 has the ballooning or the translational symmetry,[10] and is also invariant under the combined inversion $k \to -k, \lambda \to -\lambda$, which is equivalent to the CP conservation under the simultaneous reflections $r - r_0 \to -(r - r_0)$ and $\vartheta \to -\vartheta$.

It is important to note that the true 'expansion parameter' of Eq. (14) is not a simple numeric parameter like $1/n$, but an 'operator parameter' $(1/n)\partial/\partial\lambda$. As a result, the asymptotics of the system strongly depend on the mode structure in λ space. In a sense, for a consistent asymptotic analysis, the allowed wave function $\widehat{\varphi}(k,\lambda)$ must satisfy the condition $(1/n)\partial \ln \widehat{\varphi}(k,\lambda)/\partial\lambda \ll 1$. This understanding is particularly important for examining the acceptability of the plausible localized mode structures.

The expansion of the 2D wave function can be written as

$$\widehat{\varphi}_n(k,\lambda) = \Psi_n(\lambda)\chi_n(k,\lambda) + \widetilde{\varphi}_{n,1} + \cdots . \tag{16}$$

(This expansion form is adequate for the agenda of this paper. A more sophisticated expansion scheme can be found in Ref. [9]). Substituting Eq. (16) into Eq. (14) and annihilating $\widetilde{\varphi}_{n,1}$, one can obtain (up to second order in $(1/n)\partial/\partial\lambda$), the following equation for $\Psi_n(\lambda)$ [the ignored terms yield only quantitative corrections to the second order perturbation]

$$\left(i\frac{\overline{L}_1}{n}\frac{\partial}{\partial\lambda} + \frac{\overline{L}_2}{n^2}\frac{\partial^2}{\partial\lambda^2} - [\Omega - \Omega_n(\lambda)] \right) \Psi_n(\lambda) + \cdots = 0, \tag{17}$$

12

which is valid if and only if the following two conditions have been satisfied: $(\partial \ln \chi / \partial \lambda) /$ $(\partial \ln \Psi / \partial \lambda) \ll 1$ and $\xi \equiv (1/n)(\partial \ln \Psi / \partial \lambda) \approx \varepsilon \ll 1$. These constraints must be verified *a posteriori* [noting that $\partial \ln \chi / \partial \lambda \approx \mathcal{O}(1)$]. In Eq. (17), $\overline{L}_j \equiv \int dk \chi L_j \chi / \int dk \chi^2$ $(j = 1, 2)$.

Equation (17) is a differential equation to be solved subject to the periodic boundary condition: $\Psi_n(\lambda) = \Psi_n(\lambda + 2\pi)$. Notice that the λ-parameterized eigenvalue $\Omega_n(\lambda)$ (obtained by solving the ballooning equation) plays the role of a 'potential well'. Owing to the CP conservation of the ballooning equation [Eq. (15)], $\Omega_n(\lambda)$ can be approximated by

$$\Omega_n(\lambda) = \overline{\Omega}_n + \Delta \Omega_n \cos \lambda + \cdots, \tag{18}$$

because the symmetry forbids the mixing of the sines and cosine terms. One can certainly have $\cos p\lambda$ (p is an integer ≥ 2) terms without changing the essential features of the discussion to follow, if their contribution is not large [for detail, see discussion (B) of Sec. V].

We are now ready to discuss the origin of the two distinct kinds of ballooning modes, the BM-I, and the BM-II. For BM-I, or the conventional ballooning mode, one chooses only such stationary points r_0 that render $\overline{L}_1 = 0$ (the so-called solvability condition), and orders the perturbation of the eigenvalue $\Omega - \Omega_n(\lambda) \approx \mathcal{O}(\varepsilon^2)$. In the large n limit, the Mathieu equation reduces to the Weber equation for the modes localized at the extremum point λ_0, defined by $d\Omega_n(\lambda)/d\lambda \big|_{\lambda_0} = 0$. It is then straightforward to show that the small parameter $\varepsilon \approx 1/\sqrt{n}$ provides a consistent ordering, and the wave function takes the form

$$\Psi_n(\lambda) \approx \exp\left[-n\sqrt{|\Delta \Omega_n / 8 \overline{L}_2|}\, (\lambda - \lambda_0)^2\right], \tag{19}$$

where $\lambda_0 = 0$ or $\lambda_0 = \pi$, depending on the sign of $\text{Re}\{\Delta \Omega_n / \overline{L}_2\}$. Because of the highly localized nature of the eigenfunction in λ space, the eigenvalue is very close to $\Omega_0 \equiv \Omega_n + \Delta \Omega_n \cos \lambda_0$, with only a second order correction $\Omega_2 \equiv \sqrt{|\overline{L}_2 \Delta \Omega_n|/2}\, /n \approx \mathcal{O}(\varepsilon^2)$, i.e., $\Omega = \Omega_0 + \Omega_2$. The first order correction to the eigenvalue is zero for consistent ordering. Substituting $\Psi_n(\lambda)$ [Eq. (19)] back into Eqs. (12) and (13), one can directly obtain the mode structure

13

in real space. It is found that BM-I is poloidally localized at $\vartheta = 0$ (or $\vartheta = \pi$), possesses up-down symmetry in the poloidal cross-section, and is radially symmetric about r_0 with a width $\Delta r \approx r_0/\sqrt{n}$.

Recall that BM-I is subject to the solvability condition $\overline{L}_1 = 0$. Failure to satisfy this condition will deprive us of a consistent ordering which allows us to determine the mode structure by solving the second order (correct to the second order in perturbation) differential equation in λ.[10] In other words, the neglected higher order terms will become equal to or larger than the terms kept. The implication is that the BM-I type mode may not exist at an arbitrarily chosen r_0. In particular, when the system contains dissipation, the solvability condition becomes two independent constraints. It is not always possible to satisfy both of them simultaneously.[10,11] This recognition has serious consequences for applications of the conventional ballooning mode. One may wonder whether such a *localized* mode ever exists at the very radial place where it was placed for the given application.

There exists another type of solution for the system described by Eqs. (17)–(18). It applies to the radial positions where $\overline{L}_1 \neq 0$, *i.e.*, most of the radial positions. The requirement for a consistent ordering is still the same $(1/n)\partial \ln \Psi/\partial \lambda) \approx \varepsilon \ll 1$. But now with $\overline{L}_1 \neq 0$ one can neglect $(\overline{L}_2/n^2)\partial^2/\partial \lambda^2$, if $\overline{L}_2$ is of order unity. However, one must show that the solution of Eq. (17) does support such an ordering. Consistent modes obtained by solving the resulting first order differential equation will be called BM-II.

It is easy to get the solution of this first order equation

$$\Psi_n(\lambda) = \Psi_0 \exp\left(-i(n/\overline{L}_1)\int^\lambda d\lambda'[\Omega - \Omega_n(\lambda')]\right). \tag{20}$$

The periodic boundary condition on $\Psi_n(\lambda)$ leads to the determination of the eigenvalue:

$$\Omega = \oint d\lambda \Omega_n(\lambda) \to \overline{\Omega}_n, \tag{21}$$

and of the eigenfunction (mode structure)

$$\Psi_n(\lambda) = \Psi_0 \exp\left[-i(n\Delta\Omega_n/\overline{L}_1)\sin\lambda\right]. \tag{22}$$

If $\Delta\Omega_n/\overline{L}_1$ is real (non-dissipative BM-II), $\Psi_n(\lambda)$ is an oscillatory function in the λ space with an invariant amplitude. The expansion parameter of the ballooning theory, $\xi \equiv (1/n)\partial\ln\Psi_n(\lambda)/\partial\lambda \approx (\Delta\Omega_n/\overline{L}_1)\cos\lambda$, can be small only if a small parameter is inherent in $(\Delta\Omega_n/\overline{L}_1)$, because the factor $1/n$ cancels and $\cos\lambda \to \mathcal{O}(1)$. For the TAE example cited in the introduction, there is indeed a small parameter, namely the inverse aspect ratio $\widehat{\varepsilon} \equiv r/R$, that is associated with $\overline{L}_1(\overline{L}_1 = 2/q\widehat{\varepsilon})$.[8] Thus the condition $\xi \approx q\widehat{\varepsilon}\Delta\Omega_n/2 \ll 1$ is satisfied by the asymptotic smallness of $\widehat{\varepsilon}$. The radial extension of the mode can be directly calculated by making use of the standard saddle point method for integrating over λ [Eqs. (13), (16), and (22)], and turns out to be

$$\frac{\Delta r}{r_0} = \frac{\widehat{\varepsilon}\Delta\Omega_n}{\widehat{s}}. \tag{23}$$

In some papers, this Δr is emphasized as the distance between the two Wentzel-Kramers-Brillouin (WKB) turning points. The reason for this can be easily seen from the saddle point calculation. The two WKB turning points correspond to the positions where the saddle points enter into the complex plane from the real λ-axis. Outside the WKB turning points the mode falls off rapidly. In addition, the mode structure is not localized poloidally (it does not balloon) because the amplitude of $\Psi_n(\lambda)$ is invariant.[8]

It is clear now that if $\overline{L}_1$ were not asymptotically large, that is, if $\overline{L}_1$ is of order unity, neither ξ, nor $\Delta r/r_0$ could be small, unless $\Delta\Omega_n$ is small, which is precisely the case approaching the slab limit [cf. Eq. (18)]. Therefore, for real systems (or almost real systems like the weakly dissipative drift wave) another small parameter additional to $1/n$, is required for ensuring a small ξ — the condition for the validity of the asymptotic theory [large n is still necessary for Eq. (17) to be valid].

15

However, if $\Delta\Omega_n/\overline{L}_1$ is complex, and its imaginary part is not very small (dissipative BM-II), the wave function of Eq. (22) becomes localized either at $\pi/2$ ($\text{Im}\{\Delta\Omega_n/\overline{L}_1\} > 0$) or at $-\pi/2$ ($\text{Im}\{\Delta\Omega_n/\overline{L}_1\} < 0$) in the large n limit. As a result, $\cos\lambda$ contained in ξ, as well as ξ become small. The 'additional small parameter' required for the validity of the asymptotic theory will be shown to be $1/|\text{Im}\{\Delta\Omega_n/\overline{L}_1\}|n \ll 1$ (now, it is associated with n) [see what follows from Eq.(26)]. Notice that the localization of $\Psi_n(\lambda)$ can be shifted from $\lambda = \pm\pi/2$ by including even harmonics, such as $\cos 2\lambda, \cos 4\lambda, \ldots$ in $\Omega_n(\lambda)$ [cf. Eq. (18)]. Nonetheless, save for very special cases, this shift is found to be small in the numerical solutions of ballooning equation. In any case, even a sizable shift does not change the salient features of the new structure.

Substituting Eqs. (22) and (16) into Eqs. (13) and (12), one obtains by the standard saddle point method for integrating over λ,

$$\varphi_n(r, \vartheta, \zeta) = \sqrt{\frac{2\pi}{|n\Delta\Omega_n/\overline{L}_1|}} \, \exp[in\zeta - im\vartheta - i\phi_p/2] \sum_l \overline{X}_n(x - l, \sigma_\lambda\pi/2) \exp[\Phi(\sigma_\lambda)],$$

$$\Phi(\sigma_\lambda) \equiv \sigma_\lambda \left\{ -\frac{il^2}{2n\Delta\Omega_n/\overline{L}_1} - il\left(\frac{\pi}{2} + \sigma_\lambda\vartheta\right) + \frac{i\pi}{4} - in\Delta\Omega_n/\overline{L}_1 \right\},$$

$$\sigma_\lambda \equiv \text{sgn}\left[\text{Im}\{\Delta\Omega_n/\overline{L}_1\}\right], \tag{24}$$

where ϕ_p is the phase of $\Delta\Omega_n/\overline{L}_1$, $\overline{X}_n(x - l, \lambda_0)$ is the Fourier transform of $X_n(k, \lambda_0)$ with the kernel $\exp[ik(x - l)]$. Note that the λ-localization at $\sigma_\lambda\pi/2$ results in an additional factor $\sigma_\lambda l\pi/2$ in the phase $\Phi(\sigma_\lambda)$; this factor is responsible for the poloidal asymmetry of the dissipative BM-II.

The finite (not too small) $\text{Im}\{\Delta\Omega_n/\overline{L}_1\}$ makes the mode fall off rapidly with increasing $l > \overline{l}$ (a measure of the number of contributing sidebands), estimated by

$$\overline{l} \approx |\Delta\Omega_n/\overline{L}_1|\sqrt{n/|\text{Im}\{\Delta\Omega_n/\overline{L}_1\}|} \ll m \tag{25}$$

in the large n limit. This estimate of the l-width of the mode implies a radial mode width

(by taking $x \to \bar{x} \approx \bar{l}$)

$$\frac{\Delta r}{r_0} \approx \frac{1}{q\hat{s}} \frac{|\Delta\Omega_n/\bar{L}_1|}{\sqrt{n|\operatorname{Im}\{\Delta\Omega_n/\bar{L}_1\}|}}. \tag{26}$$

Comparing Eq. (26) with Eq. (23), one can readily see that a more precise meaning of the phrase 'not too small $\operatorname{Im}\{\Delta\Omega_n/\bar{L}_1\}$' turns out to be the inequality $|\operatorname{Im}\{\Delta\Omega_n/\bar{L}_1\}| \gg 1/n$. When this condition is satisfied, the mode structure is essentially described by Eq. (24). It must be emphasized that finite dissipation is crucial for a strong radial localization (small radial width) as well as for the consistency of the dissipative BM-II. The poloidal structure can also be identified from Eq. (24). For $\operatorname{Im}\{\Delta\Omega_n/\bar{L}_1\} > 0$ (< 0) the mode is localized at $\vartheta = -\pi/2$ ($\vartheta = \pi/2$). The poloidal asymmetry is attributed to the strong CP violation arising from the $\pi/2$-localization in λ.

For the reader's convenience an alternative expression for the mode structure, where the radial dependence is more explicit, is also presented. The new expression is derived by first using the Poisson formula to carry out the l sum,

$$\varphi_n(r, \vartheta, \zeta) = \exp[in\zeta - im\vartheta] \sum_p \exp[ix(2\pi p - \vartheta)]$$

$$\cdot \oint d\lambda \chi_n(2\pi p - \lambda - \vartheta, \lambda) \exp[-inq\hat{s}(y\lambda + \beta_n \sin\lambda)], \tag{27}$$

where $x \equiv nq'(r - r_0), y \equiv (r - r_0)/r_0, \beta_n \equiv \Delta\Omega_n/\bar{L}_1 q\hat{s}$. Then, the λ integral is done by the standard saddle point method to arrive at $[\operatorname{Im}\{\beta_n\} > 0]$

$$\varphi_n(r, \vartheta, \zeta) \approx \exp\left[-im\vartheta - inq\hat{s}y^2/2\beta_n\right] \sum_l \exp[il(\vartheta + \pi/2)]\bar{\chi}_n(x - l, \pi/2). \tag{28}$$

It is obvious from Eq. (28) that the radial envelope is described by the exponential factor containing y^2, that yields the same radial width as given by Eq. (26). However, Eq. (28) is not fully identical to Eq. (24). This discrepancy is probably due to the differences caused by different approximations used to sum and to integrate. For the purpose of calculating Reynolds stress, however, this discrepancy is unimportant.

17

To conclude this section it is worth making a few remarks upon CP symmetry breaking of the dissipative BM-II. As mentioned in the introduction, the original 2D eigenmode equation conserves CP to the lowest order (and in fact to the lowest order only); to this order, it is invariant under the simultaneous spatial inversion: $r - r_0 \rightarrow -(r - r_0)$ and $\vartheta \rightarrow \vartheta$ [Eq. (14)]. However, the 2D mode structure is determined by higher order terms. Thus the structure of the complete mode may or may not conserve CP. It does for BM-I for which $\overline{L}_1 = 0$ (this is the condition for BM-I to be valid) making Eq. (14) to be CP invariant to the next nontrivial (second) order required to determine the structure of the mode. For BM-II, however, $\overline{L}_1 \neq 0$, and the next leading order (first, in this case) equation does not respect CP- the CP symmetry is broken. For the non-dissipative BM-II, the CP violation merely yields an unimportant phase shift, because $\Delta \Omega_n / \overline{L}_1$ in Eq. (22) is real. In contrast, for the dissipative BM-II, the CP violation results in a strong variation of the mode amplitude in λ, and consequently causes the mode to be radially asymmetric, and to be strongly localized in the poloidal direction. The validity of the non-dissipative BM-II is guaranteed by the condition that $|\Delta \Omega_n / \overline{L}_1| \ll 1$, while $|\text{Im}\{\Delta \Omega_n / \overline{L}_1\}| \gg 1/n$ is required for the dissipative BM-II to be consistent. If neither of these conditions is satisfied, the BM-II structure cannot provide a *possible basis for a theory of localized modes in an axisymmetric torus.*

IV.   REYNOLDS STRESS FOR DISSIPATIVE BALLOONING MODES

In this section it is demonstrated that the radial asymmetry inherent in the dissipative BM-II greatly enhances their contribution to the Reynolds stress. Treatments, which ignore this feature, are likely to make a severe underestimate of the generated stress.

We continue to work within the framework of the quasilinear notion that the correlation occurs only amongst the components of a single toroidal mode; identical approach was followed for the slab model calculations in Sec. II. For a given rational surface r_j, and a

given toroidal mode number n, consider a single dissipative BM-II extending over $2l \geq 2\bar{l}$ [cf. Eq. (25)] rational surfaces. Since the radially extended wave is still characterized by the equilibrium at r_j, the mode can be viewed as pertaining to the rational surface r_j. In what follows, the modes pertaining to different rational surfaces will be assumed to be decorrelated, and so will be the modes pertaining to the same rational surface, but with different mode number n.

Consider a single mode n pertaining to the rational surface r_j. For simplicity, we drop explicit r_j-labeling before summing up the contribution from all rational surfaces. According to Eq. (24), the physical mode can be written as

$$\varphi_n(r, \vartheta, \zeta, t) = \sum_l \left\{ \overline{X}_n(x - l, \sigma_\lambda \pi/2) \cdot \exp[-i\omega t + i\widehat{\Phi}(\sigma_\lambda)] + \text{c.c.} \right\},$$

$$\widehat{\Phi}(\sigma_\lambda) \equiv n\zeta - (m + l)\vartheta - \sigma_\lambda \left[\frac{l^2}{2q\widehat{s}n\beta_n} + l\pi/2 \right],$$

(29)

where $x \equiv n[q(r) - q(r_j)] \approx nq'(r - r_j), \beta_n \equiv \beta_n(r_j), q \equiv q(r_j), m \equiv nq(r_j)$ etc. Upon defining $\overline{X}_n(x - l, \sigma_\lambda \pi/2) \equiv |\overline{X}_n(x - l, \sigma_\lambda \pi/2)| \exp(iS)$, Eq. (29) is rewritten as

$$\varphi_n(r, \vartheta, \zeta, t) = \sum_l |\overline{X}_n(x - l, \sigma_\lambda \pi/2)| \exp\left(-\frac{\sigma_\lambda l^2 \operatorname{Im}\{\beta_n\}}{2q\widehat{s}n|\beta_n|^2} \right) \cos\left(\omega t - \operatorname{Re}\{\widehat{\Phi}(\sigma_\lambda)\} - S \right). \quad (30)$$

The poloidal average on the Reynolds stress is given by

$$\mathcal{R}_j \rightarrow \left\langle \frac{1}{r} \frac{\partial \varphi_n}{\partial \vartheta} \cdot \frac{\partial \varphi_n}{\partial r} \right\rangle_\vartheta = \sum_l |\overline{X}_n(x - l, \sigma_\lambda \pi/2)|^2 \exp\left(-\frac{\sigma_\lambda l^2 \operatorname{Im}\{\beta_n\}}{q\widehat{s}n|\beta_n|^2} \right) \frac{(m + l)}{2r} \frac{dS}{dr}. \quad (31)$$

To continue the calculation, we now invoke the standard and very important model of the dissipative drift wave. The model equation describing the 2D drift wave [mode number n, and localized at the rational surface r_0] is

$$\left\{ (\rho_s k_\vartheta \widehat{s})^2 \frac{\partial^2}{\partial x^2} - \frac{\overline{\omega}_s^2}{\omega^2} \left[inq(r) + \frac{\partial}{\partial \vartheta} \right]^2 - \left(1 + \rho_s^2 k_\vartheta^2 - i\delta_e - \frac{\widehat{\omega}_e^*}{\omega} \right) \right.$$

$$\left. + 2 \frac{\omega_{de}}{\omega} \left(\cos\vartheta + i\widehat{s}\sin\vartheta \frac{\partial}{\partial x} \right) \right\} \Phi_n(r, \vartheta) = 0, \quad (32)$$

19

where $\omega_{de} \equiv T_e c k_\vartheta / eBR$, $k_\vartheta \equiv nq/r_0 \equiv m/r_0$, $nq(r) \equiv m + x$, $x \equiv nq'(r - r_0)$, $\bar{\omega}_s \equiv c_s/qR$, $\widehat{\omega}_e^* \equiv \omega_e^*(i/nq)\partial/\partial\vartheta$ with $\omega_e^* \equiv T_e c k_\vartheta / eBL_n$. In Eq. (32) the ballooning symmetry [translational invariance] breaking arises only from $\widehat{\omega}_e^*$. For the Fourier transformed field $\phi_{n,l}(x)$, defined by $\Phi_n(r,\vartheta) \equiv \exp(-im\vartheta)\sum_l \exp(-il\vartheta)\phi_{n,l}(r)$, $\widehat{\omega}_e^*$ becomes $\omega_e^*(1 + l/m)$, in which l/m violates the translational invariance. This form, in fact, is qualitatively equivalent to other choice for $\widehat{\omega}_e^*$, e.g., $\widehat{\omega}_e^* \to \omega_e^*(1 + gx/m)$ with $g \approx \mathcal{O}(1)$, because $(x - l)/n$ is of higher order compared to l/n. With these definitions, one can now manipulate Eq. (32) to derive the equivalent of Eqs. (14)–(15) keeping terms only to the first order in perturbation. The required equations are

$$L_0 = \frac{1}{\eta^2}\frac{\partial^2}{\partial k^2} + \eta^2 k^2 - \frac{2q}{\widehat{s}}\left[\cos(k + \lambda) + \widehat{s}k\sin(k + \lambda)\right], \qquad L_1 = L_s/qL_n,$$

$$\Omega = (L_s/L_n)(1 + i\delta_e - \omega/\omega_e^*), \quad \Omega_n(\lambda) = (L_s/L_n)(1 + i\delta_e - \omega(\lambda)/\omega_e^*),$$

(33)

where $\eta^2 \equiv \omega\rho_s k_\vartheta \widehat{s}/\bar{\omega}_s$ $(\eta \approx \rho_s k_\vartheta \widehat{s}\sqrt{L_s/L_n})$. At $\lambda \equiv \sigma_\lambda \pi/2$ $(\sigma_\lambda = \pm 1)$ the ballooning equation (leading order) becomes

$$\left[\frac{1}{\eta^2}\frac{d^2}{dk^2} + V(k) - \Omega(\sigma_\lambda)\right]\chi(k, \sigma_\lambda\pi/2) = 0,$$

(34)

where $V(k) \equiv \eta^2 k^2 + \sigma[\sin k - \widehat{s}k\cos k]$, and $\sigma \equiv \sigma_\lambda(2q/\widehat{s})$. Notice that under the reflection $k \to -k$, the toroidal term of Eq. (34) has opposite parity to the standard 'slab' terms. It is this parity violation that results in the radial asymmetry of $\overline{X}(x - l, \sigma_\lambda\pi/2)$. The general analytical solution of Eq. (34) is difficult. A few examples in restricted parameter regimes suffice for illustration.

For $V(k)$ expanded at k_0, defined by $\partial V/\partial k|_{k_0} = 0$, Eq. (34) becomes

$$\left[\frac{1}{\eta^2}\frac{d^2}{dk^2} + V(k_0) + \frac{V''(k_0)}{2}(k - k_0)^2 - \Omega(\sigma_\lambda)\right]\chi(k, \sigma_\lambda\pi/2) = 0,$$

(35)

with the solution

$$\chi = \chi_0 \exp\left[-\eta\sqrt{-V''(k_0)/2}\,(k - k_0)^2/2\right], \Omega(\sigma_\lambda) = V(k_0) - \sqrt{-V''(k_0)/2}\,/\eta,$$

(36)

20

provided that

$$\mathrm{Re}\left\{\eta\sqrt{-V''(k_0)/2}\right\} > 1, \tag{37}$$

which must be verified *a posteriori*. The equation

$$k_0(2\eta^2 + \sigma\widehat{s}\sin k_0) = \sigma(\widehat{s} - 1)\cos k_0 \tag{38}$$

must be solved to find k_0. The solution can be easily obtained for $\widehat{s} - 1 \equiv \Delta\widehat{s} \ll 1$. For the Pearlstein-Berk branch[14]

$$k_0 = \sigma\Delta\widehat{s}/2\eta^2 \quad (|k_0| < 1), \quad \sqrt{-V''(k_0)/2} \to -i\eta, \quad \chi \approx \exp[i\eta^2(k - k_0)^2/2],$$

and

$$\omega(\sigma_\lambda)/\omega_e^* = 1 + i(\delta_e - L_n/L_s) + \cdots .$$

The self-consistent condition [Eq. (37)] is likely to be satisfied when $\delta_e - L_n/L_s(> 0)$ is not too small, $\eta \approx \rho_s k_\vartheta \widehat{s}\sqrt{L_s/L_n} > 1$, and σ is not too large. The Fourier transformed $\overline{X}$ is

$$\overline{X}(x - l, \sigma_\lambda) \approx \exp\left[ik_0(x - l) - i(x - l)^2/2\eta^2\right]. \tag{39}$$

For the Chen-Cheng branch[15]

$$k_0 = -2\eta^2/\sigma \quad (|k_0| < 1), \quad \sqrt{-V''(k_0)/2} \to \eta, \quad \chi \approx \exp[-\eta^2(k - k_0)^2/2],$$

and

$$\omega(\sigma_\lambda)/\omega_e^* = 1 + i\delta_e + \cdots ,$$

for which the shear stabilization disappears. The self-consistent condition is likely to be satisfied in the large σ limit, so that $\eta > 1$ and $\eta^2/\sigma < 1$ hold simultaneously. The Fourier transformed $\overline{X}$ is

$$\overline{X}(x - l, \sigma_\lambda) \approx \exp\left[ik_0(x - l) - (x - l)^2/2\eta^2\right]. \tag{40}$$

The leading contribution to dS/dr (therefore, to the Reynolds stress) is found to equal $nq'k_0$ for both the branches. Because dS/dr ($nq'k_0$) turns out to be independent of l, Eq. (31) can be approximated by (for $l < m$)

$$\mathcal{R}_j \approx \frac{m}{2r}\frac{dS}{dr}\sum_l \left|\overline{X}_n(x-l,\sigma_\lambda\pi/2)\right|^2 \exp\left(-\frac{\sigma_\lambda l^2 \,\mathrm{Im}\{\beta_n\}}{q\widehat{s}n|\beta_n|^2}\right) = k_\vartheta \frac{dS}{dr}\left\langle|\varphi_n(r)|^2\right\rangle, \qquad (41)$$

where use is made of Eq. (30) to show that $\left\langle|\varphi_n(r)|^2\right\rangle$ is the ensemble average of φ_n^2.

At this stage it is worth comparing Eq. (41) with Eq. (4). The radial gradient of the phase dS/dr in Eq. (41) has the same physical content as the gradient ($d\delta_p/dr$) in Eq. (4). In magnitude these two are comparable, for $dS/dr = k_\vartheta k_0 \le k_\vartheta$, and $d\delta_p/dr \approx \sqrt{L_n/L_s\delta_e}/\rho_s \approx 1/\delta_e\Delta_r$, where Δ_r is the radial width of the slab drift wave. However, dS/dr possesses the same sign on each side of the rational surface r_j, in contrast to $d\delta_p/dr$, which changes sign as we cross the rational surface r_j. The toroidal coupling substantially modifies the mode structure by altering the phases of the local 'slab' modes in such a manner that the radial energy flow pertaining to a single toroidal mode peaked at its appropriate rational surface has a unique sense — it is either everywhere inward or everywhere outward from the entire region where the mode resides.

The Reynolds stress contributed from all rational surfaces can be easily obtained.

$$\mathcal{R} = \sum_j \mathcal{R}_j \approx \frac{\sqrt{\pi}}{2}k_0 k_\theta^3 \Delta r \varphi_n^2(r), \qquad (42)$$

where Δr is the radial envelope width given by Eq. (26). The summation over all mode numbers just replaces $\varphi_n^2(r)$ in Eq. (42) by $\varphi^2(r)$, where $\varphi(r)$ is the wave amplitude at r; all other quantities are estimated for the most probable n. The corresponding poloidal torque

$$T_{q[b]}(r) \approx \frac{\sqrt{\pi}\rho}{2}\left(\frac{c}{B}\right)^2 k_0 k_\vartheta^3 \left(\frac{\Delta r}{L_f}\right)\varphi^2(r), \qquad (43)$$

gains a factor about $(\Delta r)L_f/\Delta_r^2$ [for $\sqrt{\delta_e}\,k_y\Delta_r > 1$, it is reasonable to estimate $\delta_e k_y\Delta_r \approx 1$, k_0 has been taken to be $\mathcal{O}(1)$ in the estimate] over the slab-model torque $T_{q[s]}$ given by Eq. (7).

Now, let us compare $T_{q[b]}$ with $T_{q[DK]}$. The ratio $T_{q[b]}/T_{q[DK]}$ is $(L_s\rho_s^2 k_\vartheta^2/L_n)(\Delta r/L_f)$. Since $L_s\rho_s^2 k_\vartheta^2/L_n > 1$, this ratio may approach order unity.

At the tokamak edge, where L_f is relatively small and the nature of the modes is likely to be dissipative, the above results indicate that the poloidal torque induced by the Reynolds stress constructed by the dissipative BM-II may emerge as an important driving force for the generation of poloidal flow.

V. DISCUSSIONS AND CONCLUSIONS

The principal content of the present paper is composed of the following three major parts:

(A) A calculation of Reynolds stress incorporating the 'pairing' mechanism is given. In this part it is shown that, for the slab drift wave, cancellations brought about by 'pairing' leads to a much smaller Reynolds stress than the estimate given by Diamond and Kim. Therefore, the poloidal torque induced by the Reynolds stress constructed from the generic slab drift wave is much smaller than the driving force required for the DIII-D experiments. However, when an odd-parity driving is included in the drift wave model, the Reynolds stress can be greatly enhanced. This has been shown for the parallel flow shear driven mode, and is also possibly true for the drift-rippling mode. The odd-parity drive leads to an intrinsic radial asymmetry of mode structure causing the radial energy flow of a single mode to have a resultant component either inwards or outwards. This radial asymmetry greatly suppresses the cancellation due to 'pairing.'

(B) A brief review of the theory of 2D eigenmodes (ballooning theory) is given. In addition to presenting their rational taxonomy, we have also derived and discussed an interesting new structure, the dissipative BM-II. It is shown that for both BM-I and the non-dissipative BM-II, the fluctuation generated Reynolds stress is unlikely to be significant. This is because the combined parity, CP, is either conserved (BM-I) or its violation is weak (non-dissipative

23

BM-II), and it is the CP violation that leads to radial asymmetry, and ultimately to the creation of a sizable stress. For the dissipative BM-II the CP-violation is strong. Interestingly enough, the strong CP-violation turns out to be precisely the condition for the validity of the asymptotic theory, i.e., the $\pi/2$-localization in λ. This localization is what leads to the localization of the mode in real space [Eq. (25) and Eq. (26)]. In fact, the broken CP symmetry results in strong poloidal localization at $\vartheta = \pi/2$ (or $\vartheta = -\pi/2$) (up-down asymmetry on poloidal cross section) and a strong radial asymmetry with respect to the rational surface. Because the structure of BM-II is radially highly localized, and it can occur at all radii, its application to other topics of turbulence should also be very interesting. For example, the transport induced by the trapped particle modes of dissipative BM-II variety, could be quite different from that induced by the conventional trapped particle modes, because on one hand, most trapped particles are localized at $\vartheta = 0$, rather than $\vartheta = \pi/2$ (or $\vartheta = -\pi/2$), while on the other hand, the conventional trapped particle modes are BM-I, and may occur at very limited radial positions.

Throughout this paper our derivation of the poloidal localization for both BM-I ($\vartheta = 0, \pi$), and the dissipative BM-II ($\vartheta = \pm\pi/2$) is based on a model $\Omega_n(\lambda)$ [Eq. (18)] containing only one harmonic term. This, indeed, is found to be a rather good approximation to many numerical solutions of the ballooning equation [$\Omega_n(\lambda)$ is the eigenvalue in the ballooning equation]. However, in some special parameter regimes there can be non-negligible contribution to $\Omega_n(\lambda)$ from higher harmonics such as $\cos 2\lambda, \cos 3\lambda, \ldots$. Its effect on BM-I tends to create new extrema besides $\theta = 0$ and π. Its effect on dissipative BM-II tends either to shift the localization from $\vartheta = \pm\pi/2$, or to broaden the localization in λ, or both. The higher order ballooning theory for these cases deserves further investigation.

Some additional clarifying remarks are in order. Throughout this paper, CP-conservation (violation) very often refers to the simultaneous CP behavior of the linear equation and the modes. These two are identical within the framework of the quasilinear theory. Rigorously

24

speaking, the generation of significant Reynolds stress is associated with the CP violation of mode (amplitude) alone. In such a sense, we can not generally rule out the possible importance of BM-I with extrema in addition to $(0, \pi)$ for significant contribution to the Reynold stress, when a nonlinear symmetry breaking mechanism (if there is any) is introduced; this discussion is not covered in this paper.

(C) Finally, we present a calculation of the Reynolds stress and the induced poloidal torque generated by the toroidal drift wave of the dissipative BM-II type. It is shown that the Reynolds stress is greatly enhanced by the strong radial asymmetry inherent in this new structure associated with the dissipative BM-II. Although the calculation is restricted to limited parameter regimes of the drift wave, its generalization to other parameter regimes and to other waves is straightforward. From the manipulations for the drift wave in Sec. IV, it is readily seen that the final result [Eq. (43)] is somewhat universal (with the exception of the factor k_0 and the approximation $\hat{s} = 1$) for various kinds of modes. For a rough estimate, k_0 can be taken of order unity [notice that this is possible only if there is a significant toroidal coupling term]. However, the sign of the torque is sensitive to k_0, which is proportional to σ_λ, the signature of the poloidal localization at $\vartheta = -\sigma_\lambda \pi/2$. With these rather minor caveats, Eq. (43) can serve as a generic or a 'universal' estimate for the poloidal torque originating from the electrostatic dissipative BM-II type fluctuations. A similar formula can be constructed to estimate the poloidal torque induced by the magnetic Reynolds stress. It follows from Eqs. (1), (2), and (43) that for the electromagnetic dissipative BM-II, the torque should be of the form

$$T^{(m)}_{q[b]}(r) \approx \frac{1}{8\sqrt{\pi}} k_0 k_\vartheta^3 \left(\frac{\Delta r}{L_f} \right) \psi^2(r). \tag{44}$$

The above results indicate that substantial toroidal coupling induces significant Reynolds stress for a wide class of dissipative modes at the tokamak edge.

We end this paper by putting the present work in perspective. We are, by no means,

25

proposing that the turbulent Reynolds stress provides the only or even the principal drive for the observed poloidal rotation; there could be other forces contributing to this process. But, we have shown that significant stresses can be built up by fluctuations with a particular 2D structure (dissipative BM-II). The poloidal torque generated by this stress (which may enhance or oppose other forces), therefore, must be included in a serious theory on the origins of the poloidal rotation.

Acknowledgments

REFERENCES

[1] R.J. Groebner, Phys. Fluids B **5**, 2343 (1993).

[2] H.L. Berk and K. Molvig, Phys. Fluids **26**, 1385 (1983).

[3] P.H. Diamond and Y.B. Kim, Phys. Fluids B **3**, 1626 (1991).

[4] J.Q. Dong, W. Horton, R.D. Bengtson, and G.X. Li, Phys. Plasmas **1**, 3250 (1994).

[5] J.W. Connor, R.J. Hastie, and J.B. Taylor, Proc. R. Soc. A **365**, 1 (1979).

[6] M.N. Rosenbluth, H.L. Berk, J.W. Van Dam, and D.M. Lindberg, Phys. Rev. Lett. **68**, 596 (1992).

[7] F. Zonca and L. Chen, Phys. Rev. Lett. **68**, 592 (1992).

[8] X.D. Zhang, Y.Z. Zhang, and S.M. Mahajan, Phys. Fluids B **5**, 1257 (1993).

[9] X.D. Zhang, Y.Z. Zhang, and S.M. Mahajan, Phys. Plasmas **1**, 331 (1994).

[10] Y.Z. Zhang and Mahajan, Phys. Lett. A **157**, 133 (1991).

[11] Y.Z. Zhang, and S.M. Mahajan, and X.D. Zhang, Phys. Fluids B **4**, 2729 (1992).

[12] R.L. Dewar, private communication; also for the 'phase space' plots showing separatrix see R.L. Dewar, J. Manickam, R.C. Grimm, and M.S. Chance, Nucl. Fusion **21**, 493 (1981), and R.L. Dewar, in *Theory of Fusion Plasmas*, A. Bondeson, E. Sindoni, and F. Troyon eds. (Soc. Ital. Fisica–Editrice Compositori, Belgium, 1988) pp. 107-122.

[13] H.L. Berk, Private Communication (personal note on Jan. 1st, 1990).

[14] L.D. Pearlstein and H.L. Berk, Phys. Rev. Lett. **23**, 220 (1969).

[15] L. Chen and C.Z. Cheng, Phys. Fluids **23**, 2242 (1980).